Finite element simulation and experimental verification of ultrasonic non-destructive inspection of defects in additively manufactured materials

Cite as: AIP Conference Proceedings **1949**, 020011 (2018); https://doi.org/10.1063/1.5031508
Published Online: 20 April 2018

H. Taheri, L. Koester, T. Bigelow, and L. J. Bond

Finite Element Simulation and Experimental Verification of Ultrasonic Non-Destructive Inspection of Defects in Additively Manufactured Materials

H. Taheri[1, a)], L. Koester[1], T. Bigelow[1], and L.J. Bond[1]

[1]*Center for Nondestructive Evaluation (CNDE), Iowa State University, Ames, Iowa*

[a)] Corresponding author: htaheri@iastate.edu

Abstract. Industrial applications of additively manufactured components are increasing quickly. Adequate quality control of the parts is necessary in ensuring safety when using these materials. Base material properties, surface conditions, as well as location and size of defects are some of the main targets for nondestructive evaluation of additively manufactured parts, and the problem of adequate characterization is compounded given the challenges of complex part geometry. Numerical modeling can allow the interplay of the various factors to be studied, which can lead to improved measurement design. This paper presents a finite element simulation verified by experimental results of ultrasonic waves scattering from flat bottom holes (FBH) in additive manufacturing materials. A focused beam immersion ultrasound transducer was used for both the modeling and simulations in the additive manufactured samples. The samples were SS17 4 PH steel samples made by laser sintering in a powder bed.

INTRODUCTION

The use of industrial applications of additively manufactured components is increasing rapidly. Consequently, quality control of the parts becomes important for safety in the use of these materials [1], [2]. Experimental nondestructive evaluation practices for these materials must be established to ensure effective quality assessment [3], [4]. To better understand the physics of the problem, including adequate descriptions of the measured ultrasonic signal, and to establish the best experimental setup for inspection, the use of numerical modeling can allow the interplay of the various factors to be studied leading to improved inspection setups. The flat bottom hole (FBH) is one of the reference/calibration standards used for ultrasonic nondestructive evaluation (NDE) and to give an equivalent flaw size [5]. In additive manufacturing an FBH can be used to represent defects in different layers in the deposition [6]. The problem of wave propagation and scattering in materials, as well as reflection and scattering from FBH has been investigated both analytically [7], [8] and numerically [9]. Krautkramer (1983) used a small flaw and a far-field approximation for studying ideal disc-shaped reflectors at normal incidence [10], [11]. However, the hole maybe larger and closer to the transducer than his theory allows. Schmerr (1989) developed a model by deriving approximate analytical expression for the average pressure received by a contact compressional wave transducer from an FBH at normal incidence in pulse-echo mode [5].

The use of finite element modeling of acoustic wave propagation in testing objects has been utilized to solve a range of problems encountered in the development and verification of testing techniques, their certification and performance evaluation [12]. The modeling allows conformation of choice made for parameters and the estimated sensitivity, accuracy, flaw detectability in the given area, the influence of anisotropy and object inhomogeneity. It can also estimate coverage for particular parameter ranges, and evaluation of resolution, flaw sizes and location

44th Annual Review of Progress in Quantitative Nondestructive Evaluation, Volume 37
AIP Conf. Proc. 1949, 020011-1–020011-13; https://doi.org/10.1063/1.5031508
Published by AIP Publishing. 978-0-7354-1644-4/$30.00

capability. However, most of the investigations are based on the assumption of a plane wave transducer [13], [14] and very few of them studied focused transducers and effect on performance of different focal length. Focused transducers have, however, been widely used in nondestructive evaluation of materials due to their advantages of giving higher transverse resolution and beam intensity. Particularly with the move to material state awareness (MSA), visualizing material characteristics enhances the capabilities for quality assessment of the material. In addition to data from ultrasound, recent developments in imaging technologies such as X-ray, Computed Tomography (CT) and neutron imaging, together with advanced image processing techniques, are giving new capabilities in material characterization [15].

In this paper, a finite element 2-D model of ultrasonic wave propagation in additive manufacturing materials generated by a focused immersion transducer is presented. The samples have FBH drilled into the samples at different depths to represent defects at different depths during the deposition process. A comparison between numerical results and experimental data is performed. This method allows the solution of complex problems that are otherwise difficult or time consuming when solved analytically. X-ray images were also used to visualize the defect in the parts, and the CT images were used give data to enable the import of the as-built internal structure of the additive manufacturing material to the finite element model.

MATERIALS AND SAMPLES

The samples material is stainless steel type 17 4 PH. The additively manufactured sample was-built from powder in a 3Dsystems Prox 300 machine at Iowa State University. The reference sample used for comparison was an SS 17 4 PH annealed plate. The samples and schematics showing the 3.8 mm (0.15") deep target hole are presented in Fig. 1. The size of the samples and location of the holes are shown in Fig. 2.

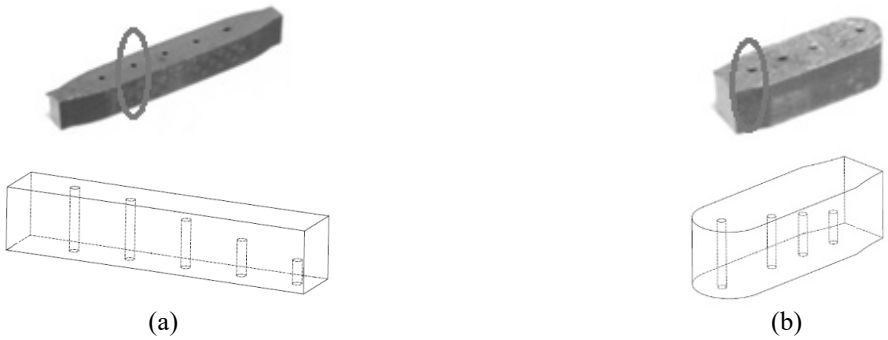

FIGURE 1. Samples with artificial flat bottom hole (FBH) defects (a) reference, and (b) additively manufactured SS 17 4 PH. 3.8 mm (0.15") deep target holes are identified by red circles.

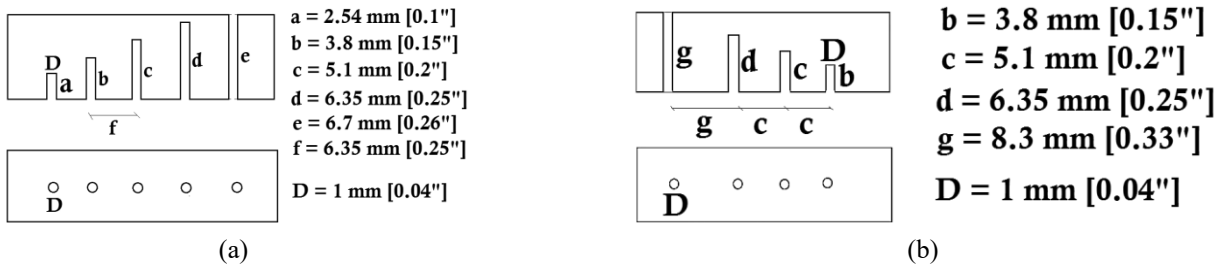

FIGURE 2. Schematic showing flat bottom holes (FBH) in (a) reference, and (b) additively manufactured SS 17 4 PH samples.

FORMULATION OF THE PROBLEM

The problem consists of modeling acoustic pressure variations in the fluid (water) domain which transfer to the solid (SS 17 4 PH) domain through a planar interface. The coupling methodology is that the fluid pressure is transmitted to the solid boundary as the normal load per unit area, and the acceleration of the solid normal to the interface is transmitted to the fluid. The governing equations for pressure acoustics in transient analysis can be written as eqn. 1 and the governing equation for solid mechanics is given as eqn. 2.

$$\frac{1}{\rho c^2}\frac{\partial^2 p}{\partial t^2} + \nabla.\left(-\frac{1}{\rho}(\nabla p - q)\right) = Q \tag{1}$$

$$\rho\frac{\partial^2 u}{\partial t^2} + d_a\frac{\partial u}{\partial t} - \nabla.\sigma = F \tag{2}$$

where, $\rho(kg/m^3)$ is the density, $c(m/s)$ is the speed of sound, $p(Pa)$ is the acoustic pressure, $t(sec)$ is the time, $q(N/m^3)$ is the dipole sound source, $Q(1/s^3)$ is the monopole sound source, $u(m)$ is the displacement in the solid, d_a is the damping coefficient, σ is the stress tensor and $F(N/m^3)$ is the body force per unit volume.

The wave propagation in each media can be calculated based on the sound speed and the distance traveled in that media. In the case of a focused transducer, the focal length will change if the wave travels through different media with different acoustic impedance (change in sound speed and density). As the ultrasonic beam propagates from the transducer through the water into the solid specimen, the beam exhibits refraction at the fluid-solid interface and results in a refocused length, $\boldsymbol{X_m}$, inside the specimen. In immersion ultrasound inspection, the new focusing point is calculated by Eqn. 3 [16]:

$$X_w = F - X_m\left(\frac{C_m}{C_w}\right) \tag{3}$$

where, X_w is the water path, F in the focusing length of the transducer, X_m is the path in the material, C_m is the sound velocity in the material and C_w is the sound velocity in water.

EXPERIMENTAL SETUP AND PROCEDURE

Experimental procedures in this study include radiography imaging and CT scanning for defect visualization, to obtain as-built structural information for the samples and ultrasonic immersion testing for defect detection and wave propagation evaluation.

Radiography and Computed Tomography (CT) Imaging

Radiography was used to visualize the defects in the samples. In addition, Computed Tomography (CT) images were taken for the additively manufactured samples and used to give data so as to be able to import the as-built porosity data into the simulation model. To evaluate the as-built condition of the drilled holes in the samples, 2D radiography images were taken from the side of the samples, which can show the depth and size of the holes. Images can be used for evaluating the as-built condition of the holes in the sample. Figure 3 shows an example of the 2D X-ray images of the samples. These examples were compared with the data for different depth holes, shown in the drawing given in Fig. 1.

(a) (b)

FIGURE 3. 2D radiography images for visualizing the target hole in (a) the reference and (b) the additively manufactured sample.

The sample, which was used for the CT imaging, is described in Fig. 4. The sample consists of a rod with a polygon (octagon) cross-section part used for the CT imaging (Fig. 4c) and a circular cross-section part used for holding the sample in the fixtures during the imaging process (Fig. 4d).

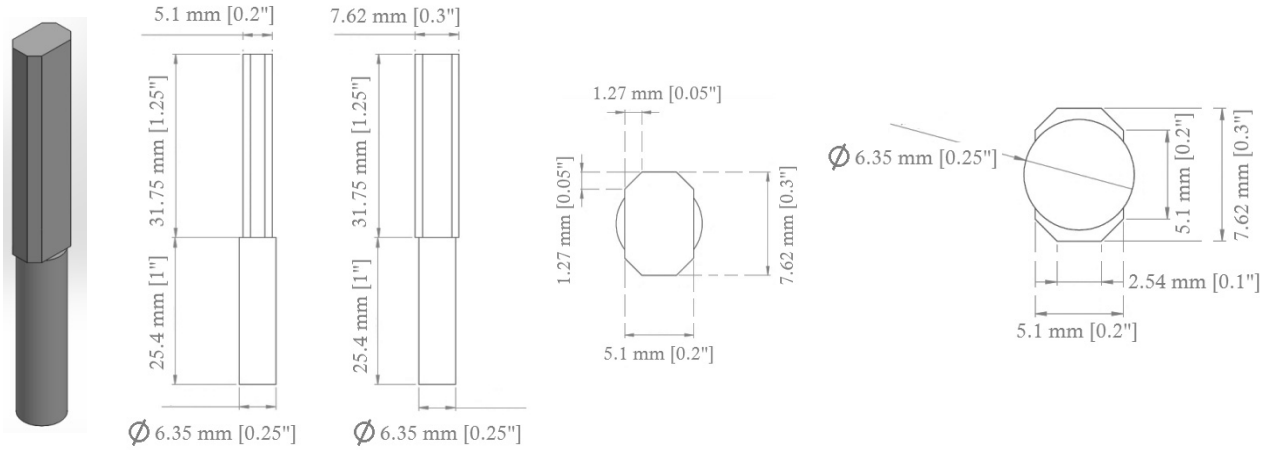

(a) (b) (c) (d)

FIGURE 4. The sample used for the CT imaging (Dimensions are in inches).

X-ray images were taken for the polygon cross-section part, and these images were used to reconstruct the CT images of the sample. The reconstructed CT image of the sample contains the as-built porosity and defect data that was imported to the FE model for simulation of wave propagation in the additively manufactured part [17], [18]. Figure 5 shows a binary 2D image (Fig. 5a) and a 3D reconstructed image (Fig. 5b) of the as-built part, where internal porosity can be seen. This model data was imported to the FEM software (COMSOL) and meshed accordingly [19].

Immersion Ultrasonic Measurements

An immersion ultrasound system was used for the experimental evaluation of ultrasound wave propagation and defect detection in both the additively manufactured and the reference samples. A schematic for the experimental system for ultrasonic immersion is shown in Fig. 6.

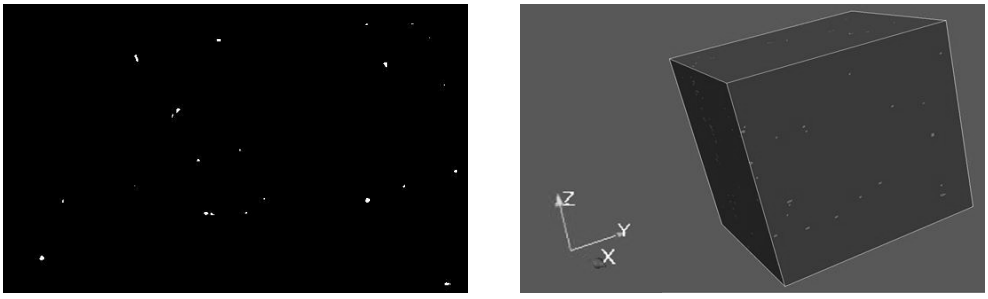

(a) (b)

FIGURE 5. The as-built SS 17 4 PH additively manufactured part: (a) binary 2D image and (b) a 3D reconstructed image.

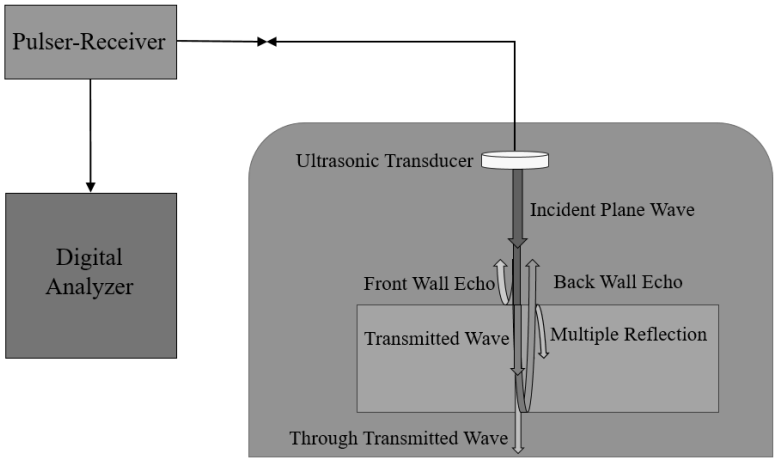

FIGURE 6. Schematic for the ultrasonic immersion experimental setup.

An ultrasonic focused immersion transducer was used for the experiments. The focal point of the transducer was set to be at two different locations, the front surface and the middle of the samples. The properties of the ultrasonic transducer are shown in Table 1. The focal point inside the material was calculated based on Eqn. 3 [16]. Ultrasonic immersion scannings of the samples were performed at these two different focal planes. The ultrasonic beam and wave parameters for the transducer are given in Table 2. All surfaces of the samples were scanned, but in this study the scattered signal from the hole with 3.8 mm (0.15 inch) length when using the 5 MHz, 50.8 mm (2 inch) focal length, transducer is considered for evaluation and to give data for comparison with the finite element model.

TABLE 1. Properties of the ultrasonic focused immersion transducer used for experiments

Transducer	Frequency (MHz)	Diameter (mm/in)	Focal length (mm/in)
Panametrics	5	12.7/0.5	50.8/2

FINITE ELEMENT MODEL AND PROPERTIES

To provide data for direct comparison with experiments, it is necessary to ensure that the Finite Element Model (FEM), the physics of the problem, appropriate geometry, material properties and boundary conditions all match the experimental data set out above.

TABLE 2. Ultrasound beam and wave parameters for the transducer used in experiments

Transducer	**Frequency (MHz)**	**Wavelength in water, $\lambda_w = \frac{C_w}{f}$ (mm)**	**Beam Diameter in water, $BD(-6\,dB) = 1.02Fc/fD$ (mm)**
Panametrics	5	0.296	1.2
Pressure wavelength in SS17 4 PH Reference sample, $\lambda_{ref,p} = \frac{C_{ref,p}}{f}$ (mm)	**Shear wavelength in SS17 4 PH Reference sample, $\lambda_{ref,s} = \frac{C_{ref,s}}{f}$ (mm)**	**Pressure wavelength in SS17 4 PH AM sample, $\lambda_{AM,p} = \frac{C_{AM,p}}{f}$ (mm)**	**Shear wavelength in SS17 4 PH AM sample, $\lambda_{AM,s} = \frac{C_{AM,s}}{f}$ (mm)**
1.176	0.624	1.146	0.632

Acoustic-Solid Interaction

Finite-element analysis was used to simulate the wave propagation in the reference and the additively manufactured SS 17 4 PH specimens with the flat bottom hole (FBH) features, with 1mm diameter and 3.8 mm (0.15 inches) depth. The model was formulated and used to simulate the 5 MHz immersion ultrasound transducer with 50.8mm (2 inches) focal length in water, with standoff adjusted to give focusing at: (a) the surface and (b) in the middle of the sample.

Materials and Geometry

The model consists of solid and water domains. Predefined material properties in COMSOL software were used for water domain. Properties for high strength steel were assigned to the solid domain and all measured properties of the samples were included in the material data used. The parameters used in the modeling are given Table 3, and the model geometry and dimensions for the 5 MHz transducer focused in the middle of the sample are shown in Fig. 7.

TABLE 3. Material properties used in the modeling

Parameter	**Water**	**SS 17 4 PH**	
		Additively Manufactured	**Reference (Annealed SS 17 4 PH plate)**
Density (kg/m^3)	1000	7737	7923
Pressure wave velocity (m/s)	1483	5730	5880
Shear wave velocity (m/s)	NA	3120	3160
Poisson's Ratio (ϑ)	NA	0.3	0.3
Width (mm)*	20	20	20
Height (Thickness) (mm)	X_w**	8.3***	6.7***

*Width of Perfectly Matching Layer (PML) = 1 mm
**Water path depends on focal length of the transducer and location of focal point in each experimental case (Eq.3)
***As for experimental conditions

Driving Pulse and Simulation Conditions

The transducer driving pulse is a decaying sinusoid pulse (Eq. 4). The interfaces between the water and steel domains are the acoustic-structure boundary. Both right and left sides of the 2D model are selected to be perfectly matched layers (PML).

$$p(t) = e^{\left(-\left(\frac{t-T}{T/2}\right)\right)^2} \times sin(2\pi f t) \tag{4}$$

where T is the pulse period, and f is the frequency. The mesh size is not larger than $\lambda/6$ and the time step for solution is obtained from Equation 5 considering CFL number of 0.2.

$$t_{step} = \frac{CFL \times L_{max}}{c} \tag{5}$$

where L_{max} is the maximum mesh size and c is the compression wave velocity. A second order triangular Lagrange element is used for meshing in COMSOL.

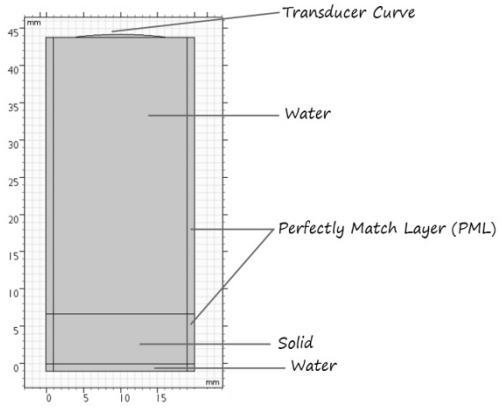

FIGURE 7. Model geometry for the 5 MHz transducer focusing at the middle of the sample.

As-built Condition for Additive Manufacturing Sample and Artificial Defect

X-ray images of the additively manufactured sample were processed to obtain the as-built condition for the porosity in the sample. These images were converted to the .DXF file format so as to be able to be imported into the FE simulation software. Figure 5a shows an X-ray image of the AM sample after image processing, which shows the as built porosity. Figure 8 shows the FE model included the AM as built material condition and the FBH 3.8 mm (0.15 inch) length in the solid domain of the model.

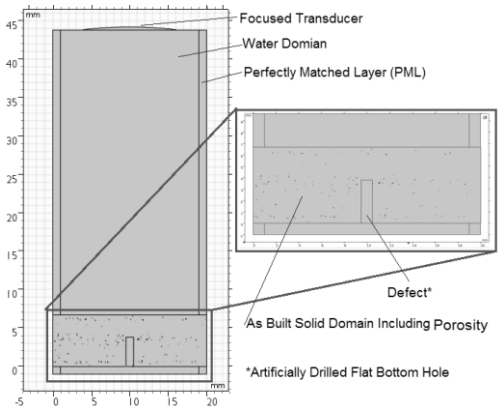

FIGURE 8. Finite element model included the AM as-built condition and the flat bottom hole 3.81 mm (0.15 inch) length in the solid domain of the model.

RESULTS AND DISCUSSION

Finite element modeling results for the ultrasound beam profile of the transducer, wave propagation and defect reflection for both the reference and AM samples at different focal planes were evaluated and data compared with the experimental results.

Finite Element Modeling Results

Figure 9 shows the beam profile of the 5 MHz focused transducer in water that was used for the experiments. Wave propagation in terms of acoustic pressure in the water domain and displacements in the solid domain are presented in Fig. 10 at the time at which the waves strike the FBH disc for the cases of (a) focusing on the surface of the reference sample (Fig. 10a) and (b) focusing in the middle of the AM sample (Fig. 10b), both for the case of the 5 MHz frequency transducer.

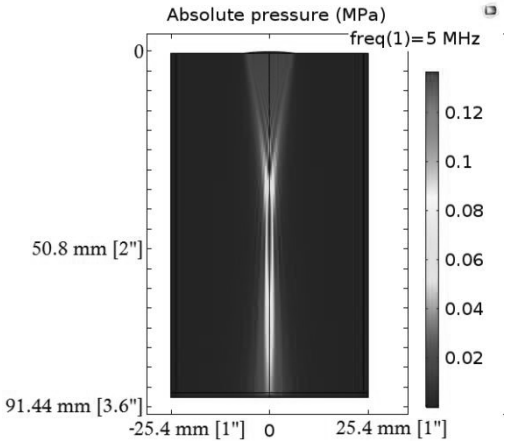

FIGURE 9. Beam profile and focusing for 5 MHz immersion ultrasound transducer with 50.8 mm (2 inch) focal length in water.

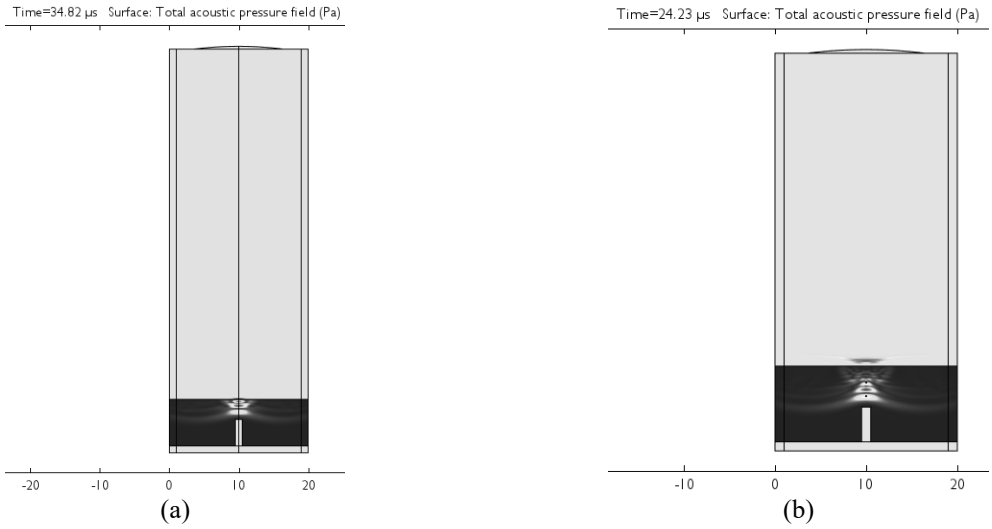

FIGURE 10. Wave propagation for 5 MHz frequency transducer for (a) focusing on the surface of reference sample, and (b) focusing at the middle of the AM samples.

Experimental Results

Ultrasonic immersion C-scan images were measured for the samples with both focusing on the front (top) surface as well as at the middle of the samples. C-scan images of the reference and additive manufacturing samples at 5 MHz frequency and with focusing on front surface and middle of the sample are shown in Fig. 11.

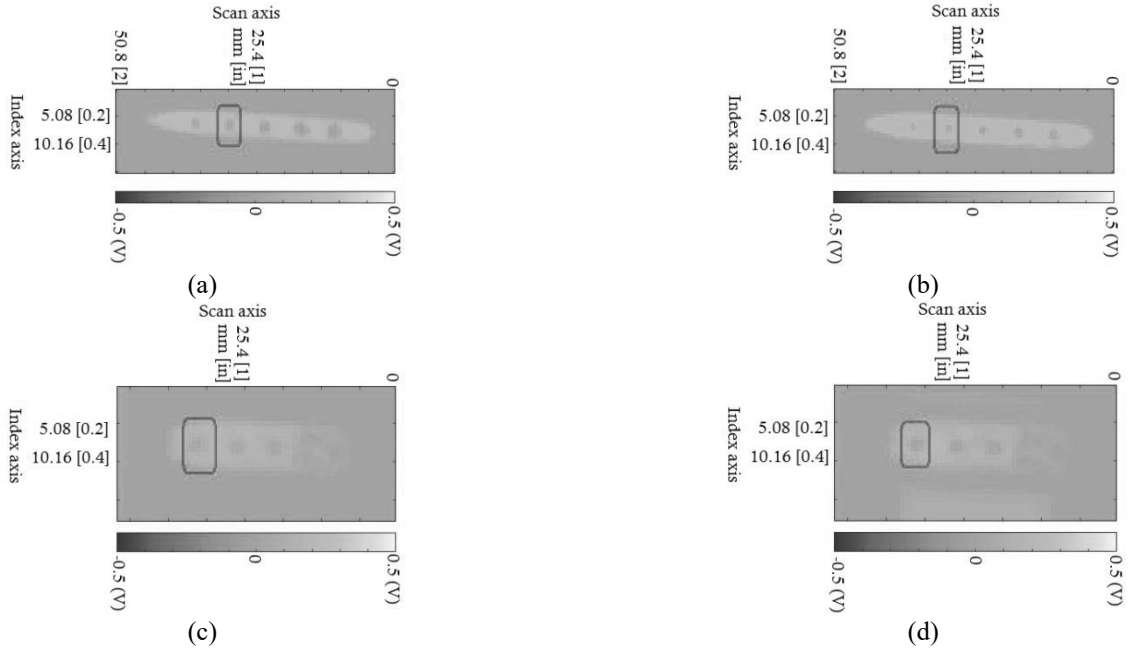

FIGURE 11. C-Scan images of the FBH in the reference and additively manufactured samples with focusing on front (top) surface and at the middle of the sample at 5 MHz frequency: (a) reference sample-focus on surface, (b) reference sample-focus at middle, (c) AM sample-focus on surface, (d) AM sample-focus at middle.

To evaluate the effect of frequency of inspection, samples were also scanned using a 15 MHz frequency transducer with 6.35mm (0.25") diameter and 25.4 mm (1") focal length. The results for the additive manufacturing sample are presented in Fig. 12 for focusing on the surface and at the middle of the sample. As can be seen from Fig. 12 and when compared with data from Fig. 11, defect detection at 15 MHz was more challenging when compared to 5 MHz. This is believed to be due to scattering caused by the effect of surface roughness on the as-built additive manufacturing sample.

FIGURE 12. C-Scan images of the defects in additive manufacturing sample with focusing on front surface and middle of the sample at 15 MHz frequency: (a) focus on surface, (b) focus at middle

Comparison of Finite Element and Experimental Results

The experimental data show that 5 MHz transducer is the better option for the inspection of FBH defects in SS 17 4 PH for both reference and additively manufactured samples. Accurate identification of the material properties as well as limitations in size of the samples and surface condition (surface roughness) are the main restrictive parameters that can limit capabilities for the precise detection of the defects. The arrival times of the signals for both cases of focusing on the surface and in the middle of the sample agree with the experimental results. However, in the experimental cases, the signals exhibit noise due to electronic devices, the measurement system and surface condition and these are the most significant factors that seem to be affecting the signal, as can be seen in Fig 12. Figure 13 shows the time of arrival of the normalized defect reflection signal for reference and AM samples respectively, while the focal point of transducer is on front wall of the samples. The flaw reflection signals from the finite element model show that the results can be used for prediction of the reflection and scattering signals from the sample and flaws. These results can be used to improve inspection procedures for a variety of similar inspection cases so as to reduce the time and cost of the inspection development.

FIGURE 13. Normalized defect reflection signal by experimental and FEM methods for (a) reference and (b) AM samples.

The effect of surface roughness on ultrasonic signals for defect detection has been developed and shows the influence of frequency and wavelength on flaw detectability [20], [21]. It has been shown that the detectability of the flaws has an inverse relationship, as compared to the optimum frequency for detection, and when the scale of roughness comes close to the wavelength, the signal distortion is higher and flaw detectability is therefore lower [20], [22]. Figure 14 shows the height map of profilometry measurement (Fig. 15a) and the height distribution model (Fig. 15b) of the roughness on the surface of the additive manufacturing sample. The average roughness value of the surface is 15.2 μm. This will influence the inspection results especially at higher frequencies as described above in the experimental section.

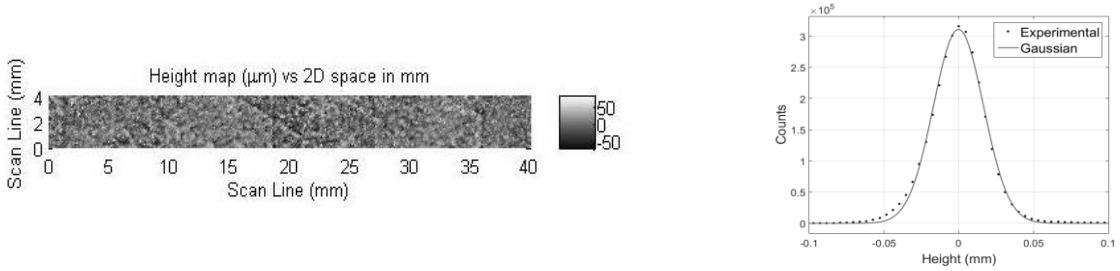

(a) (b)

FIGURE 14. Height map of profilometry measurement of the roughness on the surface of the additively manufactured sample.

Since the height distribution of the surface roughness nearly matches the Gaussian mathematical model, it can be characterized with respect to its spatial frequency content as composed of many elementary waves, and it can be represented as:

$$f(x,y) = \sum_{m=-M}^{M} \sum_{n=-N}^{N} h(m,n) \cos\big(2\pi(mx+ny) + \varphi(m,n)\big) \tag{6}$$

where; x and y are spatial coordinates, m and n are spatial frequencies, $h(m,n)$ are the amplitudes of the surface roughness, $h(m,n)$ are the phase angles. Based on surface roughness measurement, $h(m,n)$, the as-built condition of the surface can be modeled as shown in Fig. 15 for use in simulations.

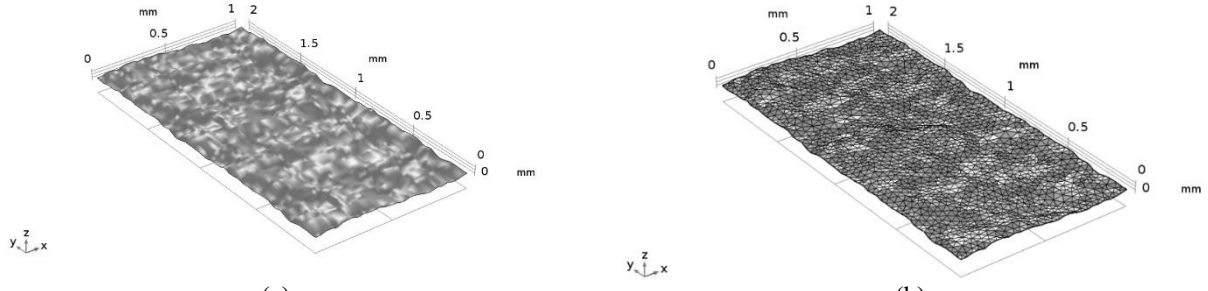

(a) (b)

FIGURE 15. Surface roughness modeling based on as-built data measurement for roughness, (a) model of the surface roughness, (b) meshed surface in COMSOL.

SUMMARY

An ultrasonic finite element (FE) model has been developed for the case of focused transducer inspection of additively manufactured materials. The model has been used to predict the ultrasonic flaw signal for FBH's. The FE element model has been extended to include the material properties and porosity of the additively manufactured sample. It has been shown that the FE approach can be considered as a tool for investigating the effects of parameters on performance and for improvement in experimental conditions to both increase the accuracy and efficiency of the inspections. The ability of the ultrasonic finite element model to predict flaw responses has been demonstrated by the comparison between the model predictions and the experimental results. The effect of focusing depth has been studied further. The results shown above indicate that inspections designed to detect FBH's in additively manufactured materials can be challenging. The selection of the inspection frequency is crucial and the experiment must be designed carefully. Moreover, if the part's surface is rough, special care must be exercised, particularly if the inspection is performed at high frequencies. For further evaluation of experimental results, more advanced signal processing techniques such as Synthetic Aperture Focusing Technique (SAFT) analysis is required. Also, 3D modeling and simulation of the problem and including surface roughness data to the model will increase the accuracy of the finite element model.

ACKNOWLEDGMENTS

This study is supported by IU Core Project at Center for Nondestructive Evaluation (CNDE), a graduated NSF IU CRC, at Iowa State University and a 2016 American Society for Nondestructive Testing (ASNT) Fellowship Award for Research in Nondestructive Testing.

REFERENCES

1. H. Taheri, M. R. Mohammad Shoaib, L. Koester, T. A. Bigelow, P. C. Collins, and L. J. Bond, "Powder based additive manufacturing - A review of types of defects, generation mechanisms, detection, property evaluation and metrology," *Int. J. of Additive and Subtractive Mater. Manuf. (IJASMM)*, **1**:2, 172-209, (2017).
2. L. Koester, H. Taheri, L. J. Bond, D. Barnard, and J. Gray, "Additive manufacturing metrology: State of the art and needs assessment," *AIP Conference Proceedings*, (eds.) D.E. Chimenti and L.J. Bond, **1706**:1, 130001, (2016).
3. M. Hasanian and C. J. Lissenden, "Assessment of coating layers on the accuracy of displacement measurement in laser Doppler vibrometry," Review of Progress in Quantitative Nondestructive Evaluation, *AIP Conference Proceedings*, (eds.) D.E. Chimenti and L.J. Bond, **1806**:1, 50006, (2017).
4. V. Chillara, H. Cho, M. Hasanian, and C. Lissenden, "Effect of Load and Temperature Changes on Nonlinear Ultrasonic Measurements: Implications for SHM," *Structural Health Monitoring 2015 System Reliability for Verification and Implementation*, (eds) F-K, Chang and F. Kopsaftopoulos, (Destech Publications, Lancaster, Pennsylvania), pp. 783-790, DOI: 10.12783/SHM2015/99, (2015).
5. L. W. Schmerr and A. Sedov, "The Scattering Response of a Flat-Bottom Hole," *Review of Progress in Quantitative Nondestructive Evaluation*, 8, (eds) D. O. Thompson and D. E. Chimenti, Plenum Publishing, New York, pp. 95-101, (1989).
6. H. Taheri, T. A. Bigelow, and L. J. Bond, "Wavefield modeling, and propagation of ultrasound for additive manufacturing materials," Technical Report, Center for NDE, Iowa State University, 2016 ASNT fellowship award, pp. 1-25, (2017).
7. A. Sedov, L. W. Schmerr, and S. J. Song, "Ultrasonic scattering by a flat-bottom hole in immersion testing: An analytical model," *J. Acoust. Soc. Am.*, **92**:1, 478-486, (1992).
8. H. Xiao, Y. Sun, D. Chen, and J. Xu, "Prediction of flat-bottom hole signals received by a spherically focused transducer for an ultrasonic pulse echo immersion testing," *Meas. Sci. Technol.*, **27**:11. 115001, (2016).
9. F. Casadei, J. J. Rimoli, and M. Ruzzene, "Multiscale finite element analysis of elastic wave scattering from localized defects," *Finite Elem. Anal. Des*. **88**, 1-15, (2014).
10. J. Krautkramer, "Determination of the size of defects by the ultrasonic impulse echo methods," *Brit. J. Appl. Phys.*, **10**, 240–245, (1959).
11. J. Krautkramer and H. Krautkramer, Ultrasonic Testing of Materials. New York: Springer-Verlag (1983).

12. K. V Petrov, O. V Muravieva, and M. A. Gabbasova, "Mathematical Modelling of the Acoustic Wave Propagation Generated by the Through-type Transducer in a Cylindrical Object," International Conference on Information Technologies in Business and Industry 2016, *IOP Conf. Series: Journal of Physics*, **803**, 012114, doi:10.1088/1742-6596/803/1/012114, (2017).
13. M. Sansalone, N. J. Nelson, and N. N. Hsu, "A Finite Element Study of the Interaction of Transient Stress Waves With Planar Flaws Flaws," *J. Res. Natl. Bur. Stand*., **92**:4, 279–290, (1987).
14. H. J. Kim, S. J. Song, and L. W. Schmerr, "Modelling ultrasonic pulse-echo signals from a flat-bottom hole in immersion testing using a multi-Gaussian beam," *J. Nondestruct. Eval*., **23**:1, 11-19, (2004).
15. K. Lynne, H. Taheri, J. Du, and F. Delfanian, "Techniques Developed for Digital Radiography and Computed Tomography Used to Advance and Evaluate the Finished Specimen," *2013 ASNT Annual Conference*, pp. 4-10 (2013).
16. L. W. J. Schmerr and S.-J. Song, Ultrasonic Nondestructive Evaluation Systems Models and Measurements. Springer, (2007).
17. B. Schneider, H. Taheri, and T. A. Bigelow, "Processing Raw CT Image Data for 2D and 3D Export into COMSOL Modelling," Technical Report, Center for Nondestructive Evaluation (CNDE), Iowa State University, Ames, Iowa, pp. 1-13, (2017).
18. B. Schneider, H. Taheri, and T. A. Bigelow, "Converting CT Scans to 2D and 3D Models for COMSOL Modelling Export Manual," Technical report, Center for Nondestructive Evaluation (CNDE), Iowa State University, Ames, Iowa, pp. 1-13, (2017).
19. COMSOL, COMSOL Inc., Burlington, Massachusetts, (2017).
20. M. Bilgen and J. H. Rose, "Ultrasonic signals from "worst-case" Hard-Alpha inclusions beneath a random rough surface," *Review of Progress in Quantitative Nondestructive Evaluation,* V.14, (eds) D.O. Thompson and D.E. Chimenti, Plenum Publishing, New York, pp. 1837-1844, (1995).
21. M. S. Greenwood, "The Effects of Surface Condition on an Ultrasonic Inspection: Engineering Studies Using Validated Computer Model," *Tech Report 11752*, NUREG/CR-6589, pp. 1-154, (Pacific NW National Lab., Richland, Washington, (1998).
22. M. Bilgen, J. H. Rose, and P. B. Nagy, "Ultrasonic Inspection, Material Noise and Surface Roughness," *Review of Progress in Quantitative Nondestructive Evaluation*, V12, (eds) D.O. Thompson and D.E. Chimenti, Plenum Publishing, New York, pp. 1767-1774, (1993).